

# Optical multiplexing of metrological time and frequency signals in a single 100 GHz-grid optical channel

P. Krehlik, Ł. Śliwczyński, *Member, IEEE*, Ł. Buczek, H. Schnatz and J. Kronjäger

**Abstract**— In this paper the concept of co-locating all metrological time and frequency signals in a single optical channel of a standard, 100 GHz-spaced optical grid is presented and evaluated. The solution is intended for situations where only a narrow optical bandwidth is available in a fiber heavily loaded with standard data traffic. We localized the optical reference signals in the middle of the channel, with signals related to RF reference and time tags shifted  $\pm 12.5$  GHz apart. In the experimental evaluation with a 260 km-long fiber we demonstrate that the stability of frequency signals and the calibration of time tags remained at the very same level of stability and accuracy as for systems utilizing separate channels: the fractional long-term instability for the optical frequency reference was below  $5 \times 10^{-20}$ , that for the RF reference at the level of  $10^{-17}$ , and the mismatch of the time tag calibration was not more than 10 ps. We also identify possible issues, mainly related to a risk of unwanted Brillouin amplification and scattering.

**Index Terms**— Time and frequency transfer, fiber optics, optical interleavers, wavelength multiplexing

## I. INTRODUCTION

THE access to precise and accurate timescales and frequency references is important for various scientific and industrial applications, such as fundamental physics, geodesy, navigation and mobile communication. However the generation of time and frequency (T&F) signals of metrological quality requires enormous investments and highly competent personnel, and is therefore only realized in a very limited number of specialized institutions around the world - usually National Metrology Institutes. Therefore remote access to these signals is very important, ideally without compromising their stability and accuracy. The

established and widely used solutions of T&F transfer (distribution) are based on satellite techniques [1]-[3]. Satellite T&F transfer is widely accessible but does not allow the accuracy and stability of the best atomic clocks and timescales to be fully exploited at the remote location, especially for the case of signals based on state-of-the-art optical clocks. Additionally, they are vulnerable to spoofing and jamming attacks, which is problematic for critical applications.

Various techniques based on optical fibers are a rapidly developing alternative [6]-[11]. However, the main problem which has to be overcome in any solution is phase (delay) fluctuations, induced in the fiber by environmental perturbations, such as temperature variations, vibrations, and mechanical stresses. In addition, to transmit a timescale, the signal propagation delay of the entire transmission system has to be known (and preferably stabilized). For these reasons, the common idea used in practically all fiber-optic T&F distribution systems is to arrange a bi-directional signal exchange in a single fiber, in order to take advantage of the high symmetry of the delay and phase fluctuations occurring in both directions. The system may operate either as a simple two-way link allowing only comparison of two remote clocks [6], or in a closed-loop phase-stabilizing scheme offering T&F distribution to the locations where no clocks are operated [8]-[11].

To transmit a coherent optical frequency reference, a continuous-wave optical carrier (OC) is transmitted via the fiber. It is derived from an ultrastable laser, which is directly referenced to an optical atomic clock by means of an optical frequency comb [13]. A radio-frequency (RF) signal (typically 10 MHz or 100 MHz) and/or a time signal (typically a pulse-per-second - 1 PPS) are usually transmitted by intensity-modulation and direct detection of the light propagating along the fiber [7], [9], [11]. As both OC and RF frequency references, together with the timescale, are generated usually at the same institutions, the idea of transferring all metrological T&F signals in some kind of combined fiber-optic system arises naturally. So far some proof-of-concept experiments have been reported, where the OC was modulated in such a way that the information carrying the RF reference and/or the time signal was combined with an optical reference. In [14], the authors demonstrated a system in which the OC was phase-modulated by pseudorandom signals produced by a commercial two-way satellite time transfer modem, routinely

Manuscript received xxxxxxx; accepted xxxxxxx. Date of publication xxxxxxx; date of current version xxxxxxx. This work was supported in part by the TiFOON 18SIB06 Project through the EMPIR Programme co-financed by the Participating States and through the European Union's Horizon 2020 Research and Innovation Program. This work was supported in part by the Polish National Science Center under the grant 2017/26/M/ST7/00128.

P. Krehlik (krehlik@agh.edu.pl), Ł. Śliwczyński, and Ł. Buczek are with AGH University of Science and Technology, Department of Computer Science, Electronics and Telecommunications, al. Mickiewicza 30, 30-059 Krakow, Poland. H. Schnatz is with Physikalisch-Technische Bundesanstalt (PTB), Quantum Optics and the Unit of Length, Bundesallee 100 D-38116 Braunschweig, Germany, and Jochen Kronjäger is with National Physical Laboratory, Time and Frequency department, Hampton Road, Teddington TW11 0LW, UK.

used for comparing remote timescales. In a proof-of-principle experiment [15], a periodically applied linear frequency chirp was applied to a transmitted, phase-stabilized OC as a means of determining the offset between timescales realized at both sides of a fiber link. In [16] and [17] the delay-stabilized transfer of multiple comb frequencies of an optical femtosecond frequency comb was proposed for simultaneous transfer of signals in the optical and the RF domain. In [18], the OC signal was amplitude-modulated in such a way that both RF and time transfer was possible. Also the concept of simultaneous transfer of two unmodulated OCs and deriving a microwave frequency reference from the difference frequency was presented in [19].

One advantage of combining the subsystems is a reduction of the optical bandwidth occupied by the metrological signal in the fiber, compared to for example using separate DWDM channels. This is paramount where T&F transfer is performed over a leased optical spectrum (due to either unavailability or cost of a dedicated dark fiber) and the optical spectrum needs to be shared with telecommunications traffic. In practice, there are also situations where a dark fiber is available for most of the planned path, but somewhere along there is a “bottleneck” where only a piece of spectrum is available. This is the case, for example, with the optical fiber link between NPL (UK) and LPL (France) [20], [21].

A general concept where regular data traffic shares the same fiber with the metrological signal (or signals) is depicted in Fig. 1. Long-haul optical networks usually utilize a dense wavelength division multiplexing (DWDM) scheme, where a large number of optical signals occupy prescribed slots of optical spectrum (optical channels). Between sections of fiber, there are data transmission nodes where the signals are processed in the optical and electrical domains. Examples of such signal processing include amplification, multiplexing and routing. Data traffic in fibers and node equipment is unidirectional, so that a pair of fibers is actually needed for full-duplex communication. Metrological T&F signals, in contrast, propagate bidirectionally within a single fiber. One possible way of introducing bidirectional metrological signals into a telecom fiber network is by inserting optical add-drop multiplexers (OADM) at the ends of each section of one of the fibers to bypass the node equipment and to provide means for bidirectional optical amplification. The role of the OADM is to separate one specific channel out (“add/drop”) for the metrological signal while passing all other channels on to the data transmission node **Błąd! Nie można odnaleźć źródła**

**odwołania.** [5].

In this paper we propose a flexible solution where the OC is optically multiplexed with RF&T signals in such a way that all signals occupy a single dense wavelength division multiplexing (DWDM) channel. The flexibility of this solution is related to the fact that optical multiplexing is fully transparent for methods used for OC phase stabilization, and also for modulation and coding schemes used for RF and time (RF&T) transfer. The only limitation is that the wavelength of the optical signals must match the passband of the OADM.

## II. PRINCIPLE OF THE OPTICAL-LAYER MULTIPLEXING OF ALL METROLOGICAL SIGNALS IN A SINGLE DWDM CHANNEL

The proposed multiplexing scheme is based on a few assumptions: (a) both the stabilized OC transfer and the stabilized RF&T transfer utilize bidirectional signal exchange for fiber noise cancellation, (b) OC signals transmitted in forward and backward directions are very close in frequency (10 MHz - 100 MHz apart) and are not optically separated (filtered) [22], [23], (c) forward and backward RF&T signals must be optically separated to eliminate backscattered and reflected light [10], [11], (d) OC signals should be separated from RF&T signals to avoid unacceptable interferences between the two metrological sub-systems. Since our goal was to allocate all signals within a single DWDM channel in a 100 GHz grid, we propose to locate the OC frequencies in the middle of the corresponding ITU channel, with RF&T forward and backward signals offset by  $\pm 12.5$  GHz. (This relatively small separation of multiplexed signals is dictated by the fact that the useful bandwidth specified for 100 GHz-grid OADMs is 27.5 GHz (0.22 nm) and their characteristics are not guaranteed out of this band.) Since commercially available thin-film or Bragg-grating filters commonly used in fiber optic telecom systems do not allow the separation of signals 12.5 GHz or even 25 GHz apart, we have used so-called optical interleavers, which were originally designed for a first stage of separation of a large number of extremely densely spaced optical data channels. The scheme showing the proposed spectral locations of the signals, together with the characteristics of the optical filters used, is depicted in Fig. 2. For historical reasons the metrological signals usually occupy DWDM channel C44 (194.400 THz), but in principle they can be located in any channel. A standard single-channel OADM is used to combine the metrological channel with all other data-carrying telecom channels (compare also Fig. 1).

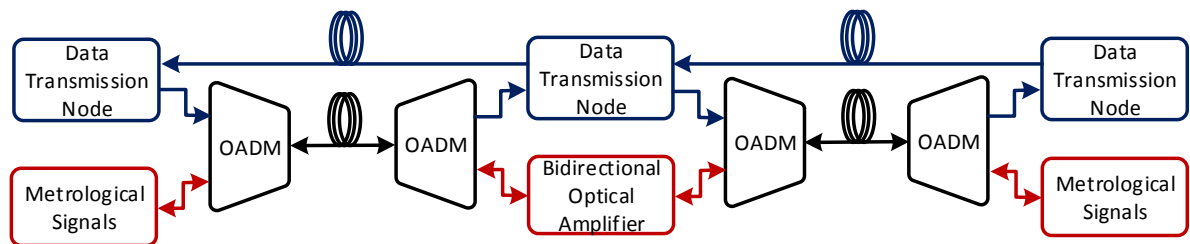


Fig. 1. General concept of multiplexing metrological signals with regular data transmission in an optical network.

> REPLACE THIS LINE WITH YOUR PAPER IDENTIFICATION NUMBER (DOUBLE-CLICK HERE TO EDIT) <

3

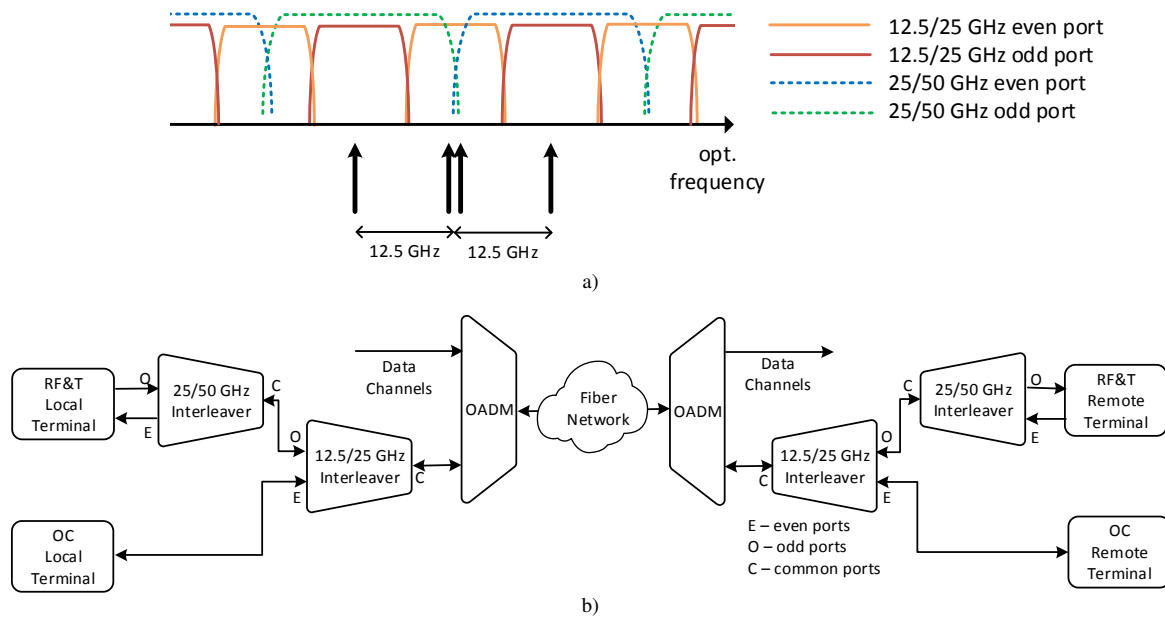


Fig. 2. (a) Interleaver passbands and relative frequencies of the metrological signals, and (b) resulting multiplexing scheme.

### III. EXPERIMENTAL EVALUATION

In the proof-of concept experimental setup, we used a typical OC transfer scheme with optical-domain active cancellation of the phase noise induced by a fiber [22], [23]. A clean-up laser phase locked to the incoming signal at the remote side (similar to the one described in [18]) acts both as a source of the return signal and as a remote output. As a subsystem for RF reference and time transfer we used ELSTAB technology [11], with noise cancellation in the electrical-domain and 1 PPS time tags embedded into 10 MHz transfer in the form of a specific phase modulation.

#### A. Interleavers characterization

In the first step we evaluated the performance of the optical interleavers, which are the key components of the proposed scheme. We used modules provided by Optoplex, based on free-space optics micro-interferometer technology with athermal design. In our application not only amplitude (transmission) characteristics, but also the group delay (dispersion) characteristics and their thermal stability are essential.

The amplitude characteristics of the evaluated interleavers are presented in Fig. 3. As one may notice, they are flat-top in a reasonable frequency range, the insertion losses in the passband are about 2–2.5 dB, and the isolation between the odd and even channels is better than 25 dB.

The measured group-delay characteristics of both types of interleavers together with the channel C44 OADM, are presented in Fig. 4. As expected, the narrower filters show the fastest change of the group delay for frequencies off the filter center. At an offset of 2 GHz from the passband center the slope is approximately 3.5 ps/GHz for the 12.5/25 GHz

interleaver, and below 1 ps/GHz for the 25/50 GHz one. The group delay change for the 100 GHz OADM is much smaller and thus is of minor importance, as long as the overall transfer characteristic of a given device is not substantially shifted from the nominal channel center. Slight shifts of the filters relative to their nominal frequency positions can be observed, but could also be caused by an offset and/or drift of the optical spectrum analyzer used for the frequency measurements. In any case, it is recommended to locate the frequency of the signal lasers in the middle of the narrower, 12.5/25 GHz interleaver passband using the same frequency measuring instrument for both interleaver characterization and tuning of the lasers.

We also examined the thermal sensitivity of the interleavers, applying 20°C temperature variations. We

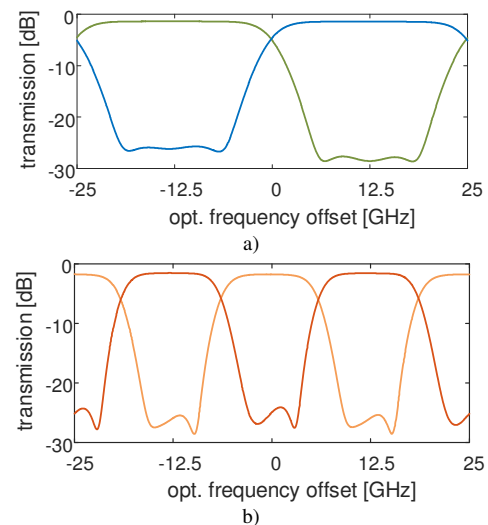


Fig. 3. Measured interleaver passbands for (a) 25/50 GHz and (b) 12.5/25 GHz devices.

> REPLACE THIS LINE WITH YOUR PAPER IDENTIFICATION NUMBER (DOUBLE-CLICK HERE TO EDIT) <

4

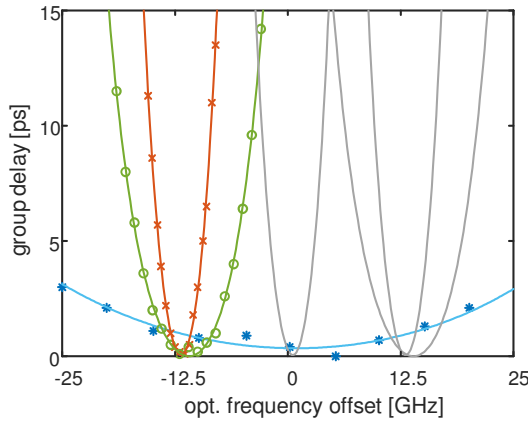


Fig. 4. Group delay characteristics of odd port of 12.5/25 GHz interleaver (red), odd port of 25/50 GHz interleaver (green), and pass port of 100 GHz OADM filter (blue). In gray we marked schematically also even port of 12.5/25 GHz interleaver (centered around zero offset), the next odd port passband of 12.5/25 GHz interleaver, and even port passband of 25/50 GHz interleaver (the last two centered around +12.5 GHz offset). For all cases group delay values are normalized to zero at the passband center.

observed a very good thermal stability, with possible shifts being comparable with the uncertainty of our measurements. (The stability specified by the manufacturer is  $\pm 1.5$  GHz in the temperature range from  $-5^{\circ}\text{C}$  to  $+65^{\circ}\text{C}$ .) However, we observed temporary shifts of about 0.5 GHz for the case of a rapid temperature slope such as  $20^{\circ}\text{C}$  per 20 minutes, which vanished in the steady state. They are probably caused by mechanical stresses related to high temperature gradients inside the interleaver package.

The final evaluation of the thermal stability of the interleavers was performed *in situ*, i.e. we observed the stability of both the optical frequency and the RF frequency transfer with one interleaver placed in a thermal chamber and the rest of the equipment kept at a stable temperature. We applied temperature cycles with  $10^{\circ}\text{C}$  amplitude and 4 hours full-cycle, and under such conditions we observed no significant degradation of the frequency stability. As an example, we show in Fig. 5 the Modified Allan Deviation, MADEV, calculated from an almost three-day measurement

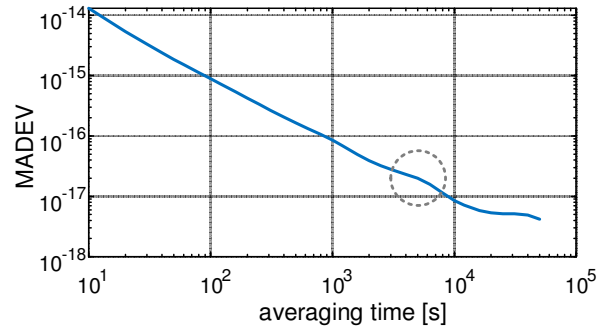


Fig. 5. The evaluation of impact of interleaver thermal sensitivity on RF transfer stability. The gray circle shows the region where the temperature cycles slightly affected stability.

of 10 MHz RF transfer with ELSTAB terminals connected with a short patchcord, a 10 dB attenuator and the 12.5/25 GHz interleaver under test placed in the optical path. If the temperature cycles had significantly influenced the group delay of the filter, the MADEV plot would have revealed a bump at an averaging time of 2 hours. As can be seen, there is only a barely noticeable bump, which means that the temperature stability of the interleaver is quite satisfactory. Similarly, we investigated the impact on stability of OC transfer, and also the impact of the 25/50 GHz interleaver on the RF stability. In all these cases, we observed no stability degradation when the interleavers were placed in the optical path.

### B. Main experiment

The main experiment was organized as shown in Fig. 6. The 25/50 GHz interleavers were embedded internally in ELSTAB terminals and played the role of directional duplexer and of a filter protecting the receiver from backscattered and reflected signals. The laser transmitters were equipped with accurate wavelength stabilization, based on wavelength lockers provided by the same manufacturer as the interleavers, with wavelength accuracy specified as better than 0.5 GHz (including aging). The optical signals generated by ELSTAB were multiplexed with the OC signals using the 12.5/25 GHz

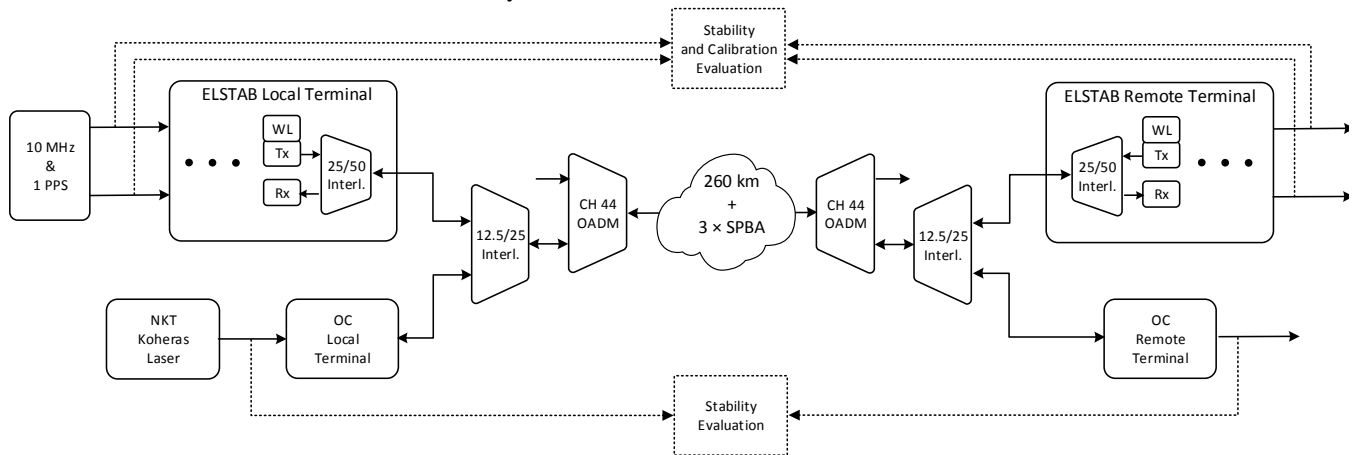


Fig. 6. Schematic diagram of the main experiment.

> REPLACE THIS LINE WITH YOUR PAPER IDENTIFICATION NUMBER (DOUBLE-CLICK HERE TO EDIT) <

5

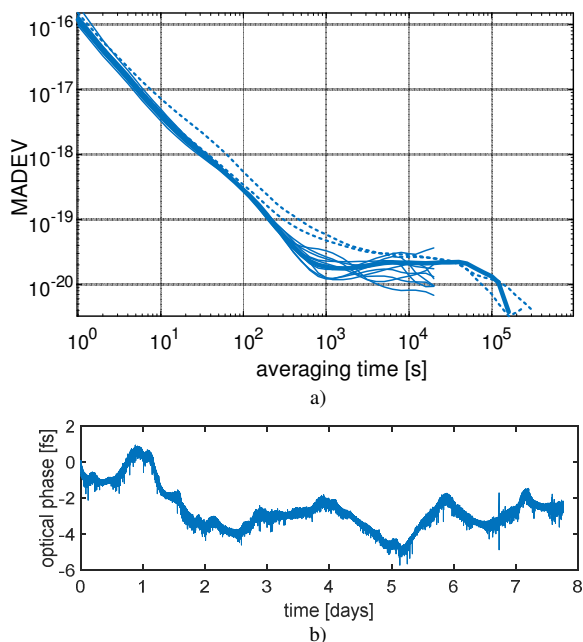


Fig. 7. (a) Modified Allan Deviation plots, and (b) time-domain evolution of the output optical phase.

interleavers. In addition, we inserted the OADM's intended for combining metrological signals with DWDM data traffic (not actually present at this experiment) (compare Fig. 1). The optical frequency transfer subsystem consists of a narrow linewidth (100 Hz), frequency stabilized fiber laser (NKT X15 Koheras), a standard phase noise cancellation setup at the local side and a clean-up laser (Rio Planex, free-running linewidth of 1 kHz) at the remote side. The clean-up laser was phase-locked to the incoming signal with 500 kHz tracking bandwidth and 60 MHz frequency offset. The optical path consisted of two 70 km-long fiber sections on spools ( $2 \times 15$  dB attenuation), two 60 km-long sections of urban fiber ( $2 \times 18$  dB attenuation, many patches and high level of acoustic noise and step-like fluctuations of the optical length), and three single-path bidirectional erbium amplifiers (SPBAs) located between the abovementioned sections.

The ELSTAB terminals and the measurement equipment for RF transfer stability and time transfer calibration measurements were located in a temperature-stabilized laboratory, whereas the rest of the equipment was installed in a laboratory without air conditioning. The only exception to this is that the fiber-based optical interferometers used in the OC subsystem and the coupler combining the local and remote optical frequency signals (for stability analysis) were placed in an aluminum box with active temperature stabilization. The stability of the transfer of both the OC and the RF frequency was measured for 33 days, starting in mid-August (i.e. well after the Covid-19 lockdown, when the acoustic noise observed in our outdoor fibers had returned to its normal level). The evaluation of the RF transfer was continuous throughout this period, while the optical frequency evaluation was interrupted by a crash of the recording computer. The continuous measurements of the OC transfer lasted 15 and 10 days.

The evaluation of the optical frequency transfer stability was performed by recording the phase fluctuations of the 20 MHz beat note between the source laser and the remote clean-up laser. During the first recording period (15 days) we observed three cycle slips, including an eight days long record without any slip. In the second period there were four cycle slips, including 2.5 days without any cycle slip. Fig. 7 a shows MADEV plots calculated from collected phase data averaged over 1 s with deadtime-free counters (K+K FXE). The thin lines are randomly selected plots calculated from one-day data, the thicker one is calculated from the eight-day period without slips, and the dashed lines are plots obtained from the full two registration periods, with the cycle slips removed from the records. As can be seen, the instability for  $10^3$  s observation time is always well below  $10^{-19}$ , and that the instability for the one-day observations is slightly above  $10^{-20}$ . Fig. 7 b shows the time-domain phase evolution in the eight-day period without cycle slips. It should be noted that there is no linear trend in the output optical phase, which means that there is no systematic frequency error. We also recorded a few days of phase data with the RF and time transfer switched off, and we have not observed any difference in stability.

The RF stability, measured similarly as in [24], is presented in Fig. 8. The MADEV smoothly decreases to  $10^{-17}$ , and the phase excursions are limited to 10 ps peak-to-peak. These results are no worse than in many previous experiments with ELSTAB terminals [11], [24], [25], so it can be concluded that normal operation of the RF transfer was achieved.

In the next step we analyzed and examined the possibility of accurate calibration of the time transfer. The calibration of the time transfer, i.e. determining the accurate value of the delay of the output time signal (output 1 PPS pulses) with respect to the input timescale (input 1 PPS pulses), is done by measuring the round-trip delay of the time signal (which should then be divided by two) and determining correction factors related to the asymmetry between forward and backward propagation [24]. One of the important factors affecting the propagation

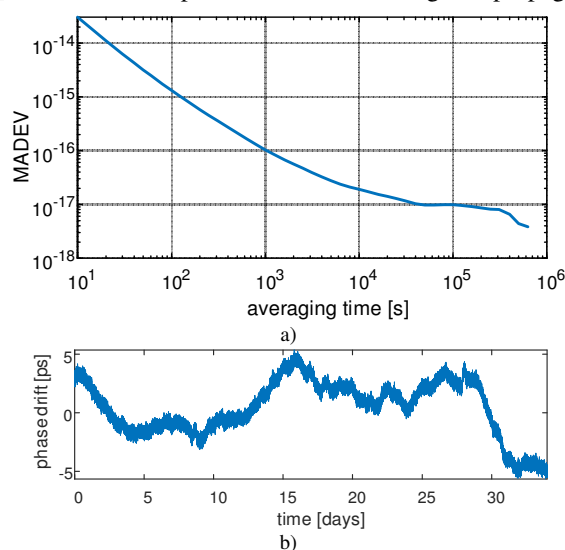


Fig. 8. (a) Modified Allan Deviation plots, and (b) time-domain evolution of the output RF phase.



> REPLACE THIS LINE WITH YOUR PAPER IDENTIFICATION NUMBER (DOUBLE-CLICK HERE TO EDIT) <

6

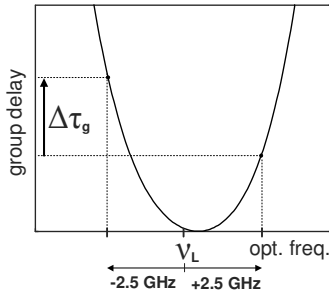


Fig. 9. Illustration of the impact of cumulated group delay characteristic of all four cascaded interleavers on time transfer calibration.

asymmetry is the chromatic dispersion of the fiber. In principle it could be measured with a special chromatic dispersion analyzer, but in practice it is very difficult to obtain reliable data from the fiber operator. Therefore, we have implemented a possibility for autonomous measurement of the dispersion-induced asymmetry in the ELSTAB terminals [26]. This is based on temporary detuning of the laser at the local side and the measurement of the resulting difference in the round-trip delay, which allows the calculation of the dispersion value. However, in the current situation where the optical signal is transmitted through four interleavers in series with rapidly varying group delay characteristics (see Fig 4), even a laser shift of a few gigahertz would result in an error of tens of picoseconds if incorrectly accounted for. The best option seems to be shifting the laser symmetrically around the nominal value and measuring the change of the round-trip delay between these two side points. However, if the group delay characteristic of the cascaded interleavers is not perfectly symmetric, and/or the (unshifted) frequency of the laser on the local side is not perfectly centered within the interleaver passband, the resulting difference in the group delay caused by the interleavers ( $\Delta\tau_g$  in Fig. 9) would affect the accuracy of the chromatic dispersion measurement. Therefore, the value of  $\Delta\tau_g$  for a given set of interleavers must be measured prior to in-field calibration and must be taken into account during the calibration procedure. The measurement of  $\Delta\tau_g$  can be performed relatively easily by detuning the laser on the local side with local and remote terminals connected with a short patchcord (and an attenuator), instead of a real fiber, because in this case only the group delay characteristics of the interleavers influence the round-trip delay. In our case  $\Delta\tau_g$  was measured to be 10.2 ps when we shifted the laser by  $\pm 2.5$  GHz. This value was then used as an additional correction factor in the calibration.

We performed a few tests of calibration accuracy by comparing the directly measured delay of the output 1 PPS pulses with the result of the calibration procedure, similarly to what we have described before in [24]. In Table 1 we present the results of comparison between the delay of the remote-side 1 PPS pulses measured directly and obtained with the calibration procedure. The results are similar to our previous experiments with RF and time transfer which were not multiplexed with optical frequency transfer [11], [24]-[26]. However, it should be emphasized that the group delay characteristics of the interleavers used in the multiplexed system must be taken into account during the time transfer calibration, and their thermal sensitivity and aging will affect the calibration accuracy.

#### IV. DISCUSSION

During the proof-of-concept experiments, described above, we observed some practical issues, which should be considered when planning operational installations, and which are therefore described below.

At some stage of our experiments, just by chance, the frequency of the NKT Koheras laser was slightly detuned with respect to the center of channel C44, and its offset from the ELSTAB backward laser was not 12.5 GHz, but approximately 10 GHz, close to the characteristic frequency offset for stimulated Brillouin amplification. Thus the ELSTAB backward laser became a Brillouin pump for the forward optical frequency signal. Even the very small residual fluctuations of the frequency of the ELSTAB laser, together with varying polarization conditions, resulted in the Brillouin amplification process being randomly switched on and off, causing power fluctuations and waveform distortion in the ELSTAB signal. As a result the phase of the RF and time transfer signal was fluctuating substantially by up to 40 ps, despite a power loss of only around 1 dB - see Fig. 10. The disproportionate effect on phase at almost negligible power loss may have been caused by removal of narrow spectral components from the modulated ELSTAB signal, causing waveform distortion. The instability visible in the figure vanished completely when we corrected the frequency of the Koheras laser and so restored the 12.5 GHz separation between OC and ELSTAB signals.

A similar problem could be caused by stimulated Brillouin scattering (SBS) of the backward optical frequency signal, especially in a long link equipped with bidirectional optical amplifiers with relatively high-gain. The SBS signal generated by the OC is relatively close to the forward ELSTAB signal

TABLE I  
VERIFICATION OF THE TIME TRANSFER CALIBRATION

Optical path length	50 km	100 km	190 km + 2 × SPBA	260 km + 3 × SPBA
1 PPS delay measured directly [ps]	249 249 028	496 819 108	953 994 213	1 298 799 301
1 PPS delay obtained by calibration [ps]	249 249 030	496 819 111	953 994 223	1 298 799 308
Difference [ps]	2	3	10	7

The expanded uncertainty estimated for the direct measurement is  $\pm 3$  ps, and for the calibration procedure is  $\pm 15$  ps.

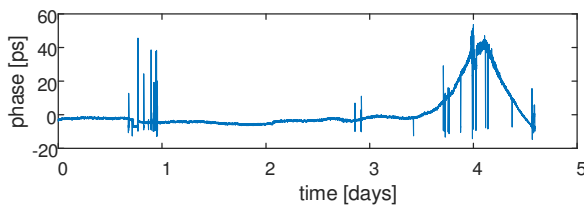


Fig. 10. Instability of RF transfer caused by the undesired stimulated Brillouin amplification.

(nominally 2.5 GHz apart) and would cause an additional interference signal in the ELSTAB receiver at the remote side. Therefore, the power of the backward OC signal must be kept at a safe level below the threshold of SBS. In our case of a 260 km-long link with three amplifiers, this safe level occurred to be -5 dBm.

The next problem that should be considered for practical installations is how to control the gain of the optical amplifiers. The sensitivity of intensity modulated fiber optic systems (as RF and time transfer) is much lower (order of -30 dBm) than that of optical frequency transfer (order of -60 dBm). Therefore, the gain of amplifiers should be chosen sufficient for the modulated signals. In principle, the easiest way to obtain the desired gain of the SPBA amplifier is to manually adjust the pump power, but in this case the gain depends on the number and power level of the signals being amplified, which is very cumbersome in practice. Therefore we implemented automatic gain control of the SPBAs, which is based on measuring the level of the modulated signals passing the amplifier. However, in this situation, the OC transfer becomes dependent on the presence of RF&T signals, which is again impractical. Finally, we arrived at the solution that in case the modulated signals vanish the automatic gain control is deactivated and a relatively low, constant pump power is applied. The resulting gain is (should be) still sufficient to meet the sensitivity requirements of the optical frequency transfer system, and on the other hand safe with respect to SBS and uncontrolled lasing of amplifiers. We investigated this solution by switching off the OC signals and observed the operation of RF&T transfer, and vice versa. In each case, the remaining subsystem operated smoothly, without re-locking or cycle slips.

## V. CONCLUSION

In this work we demonstrated the idea and a proof-of-concept experiment of a hybrid system capable of transferring all metrological signals produced in the top-level time and frequency laboratories in a single DWDM channel: the most stable and accurate optical frequency reference, the widely used 10 MHz electrical frequency reference, and a 1 PPS time signal defining the particular realization of the UTC timescale. Thanks to the active stabilization of the phase (delay) of the signals traveling down the fiber, and accurate calibration of the time transfer, the remote terminal of this system may be considered a “virtual time and frequency laboratory”, providing signals of practically the same quality as the real one feeding in the signals at the local end.

The basic motivation behind this solution was to compress all four optical signals being transmitted into a single 100 GHz-grid DWDM channel in order to minimize the optical bandwidth used for metrological time and frequency signals in a regular network with dense data traffic. In addition, another advantage of the proposed combined system would be that the ultrastable OC can be used as a reference for wavelength stabilization of lower grade semiconductor lasers carrying RF&T signals, and thus the stability and especially calibration of the time signal might be improved [27].

Although we demonstrated that the transferred frequency stability and time calibration of the solution presented here is practically the same as obtained for separate OC and RF&T transfer (without squeezing the optical signals), it should be noted that the proposed solution, although in principle quite simple and elegant, has specific requirements and limitations. First of all, the thermal and long-term stability of interleavers and wavelength lockers (used for RF&T lasers stabilization) is crucial. Then the proximity of the frequency separation (12.5 GHz) to the Brillouin scattering frequency shift (~10 GHz) means that special care is needed to avoid undesired Brillouin amplification and scattering. Last but not least, the proximity of the signals made it difficult (expensive) to separate the signals at amplification points. Therefore, there is no simple way to optimize the gains of amplifiers separately for RF&T and OC subsystems or to use quasi-bidirectional amplifiers with optical isolators preventing propagation of backscattered and reflected signals [28]-[30]. However, all these issues could be seriously relaxed if a slightly larger bandwidth could be allocated to the metrological signals (such as 200 GHz), so that the signal spacing could be increased to e.g.  $\pm 25$  GHz.

The key advantage of the optical-layer multiplexing of metrological signals when compared with systems based on modulation of the OC signal is its complete transparency with respect to particular solutions used in OC and RF&T subsystems.

## REFERENCES

- [1] W. Lewandowski, J. Azoubib, and W. J. Klepczynski, “GPS: Primary tool for time transfer,” *Proc. IEEE*, vol. 87, pp. 163–172, 1999.
- [2] G. Petit and Z. Jiang, “GPS all in view time transfer for TAI computation,” *Metrologia*, vol. 45, pp. 35–45, 2008.
- [3] D. Piester, A. Bauch, L. Breakiron, D. Matsakis, B. Blanzano, and O. Koudelka, “Time transfer with nanosecond accuracy for the realization of international atomic time,” *Metrologia*, vol. 45, pp. 185–198, 2008.
- [4] F. Kéfélian, O. Lopez, H. Jiang, C. Chardonnet, A. Amy-Klein, and G. Santarelli, “High-resolution optical frequency dissemination on a telecommunications network with data traffic,” *Opt. Lett.*, vol. 34, pp. 1573–1575, 2009.
- [5] O. Lopez et al., “Ultra-stable long distance optical frequency distribution using the Internet fiber network,” *Opt. Express*, vol. 20, pp. 23518–23526, 2012.
- [6] C. E. Calosso, E. Bertacco, D. Calonico, C. Clivati, G. A. Costanzo, M. Frettelli, F. Levi, A. Mura, and A. Gonone, “Frequency transfer via a two-way optical phase comparison on a multiplexed fiber network,” *Opt. Lett.*, vol. 39, pp. 1177–1180, 2014.
- [7] X. Chen et al., “Simultaneously precise frequency transfer and time synchronization using feed-forward compensation technique via 120 km fiber link,” *Sci. Rep.*, vol. 5, art. no 18343, 2015.

- [8] Droste et al., "Optical-frequency transfer over a single-span 1840 km fiber link," *Phys. Rev. Lett.* vol. 111, pp. 110801-5, 2013.
- [9] E. Dierikx et al., "White rabbit precision time protocol on long-distance fiber links," *IEEE Trans. Ultrason. Ferroelectr. Freq. Control*, vol. 63, pp. 945-952, 2016.
- [10] B. Wang et al., "Precise and Continuous Time and Frequency Synchronisation at the  $5 \times 10^{-19}$  Accuracy Level," *Scientific Reports*, vol. 2, 2012.
- [11] P. Krehlik, Ł. Śliwczynski, Ł. Buczek, J. Kołodziej and M. Lipiński, "ELSTAB-fiber-optic time and frequency distribution technology: a general characterization and fundamental limits," *IEEE Trans. Ultrason. Ferroelectr. Freq. Control*, vol. 63, pp. 993-1004, 2016.
- [12] S. Schediwy, D. Gozzard, S. Stobie, J. A. Malan, K. Grainge, "Stabilized microwave-frequency transfer using optical phase sensing and actuation," *Opt. Lett.*, vol. 42, pp. 1648-1651, 2017.
- [13] N. R. Newbury, W. C. Swann, "Low-noise fiber-laser frequency combs," *J. Opt. Soc. Am. B*, vol. 24, pp. 1756-1770, 2007.
- [14] O. Lopez et al., "Simultaneous remote transfer of accurate timing and optical frequency over a public fiber network," *Appl. Phys. B*, vol. 110, pp. 3-6, 2013.
- [15] S. Raupach and G. Grosche, "Chirped Frequency Transfer: A Tool for Synchronization and Time Transfer," *IEEE Trans. Ultrason., Ferroelectr., Freq. Control*, vol. 61, pp. 920-29, 2014.
- [16] S. M. Foreman, K. W. Holman, D. D. Hudson, D. J. Jones, Jun Ye, "Remote transfer of ultrastable frequency references via fiber networks," *Review of Scientific Instruments*, vol. 78, pp. 021101/1-25, 2007.
- [17] G. Marra et al., "High-resolution microwave frequency transfer over an 86-km-long optical fiber network using a mode-locked laser," *Optics Letters*, vol. 36, pp. 511-513, 2011.
- [18] P. Krehlik, H. Schnatz, Ł. Śliwczynski, "A hybrid solution for simultaneous transfer of ultrastable optical frequency, RF frequency and UTC time-tags over optical fiber," *IEEE Trans. Ultrason. Ferroel. Freq. Contr.*, vol. 64, pp. 1884-1890, 2017.
- [19] D. R. Gozzard, S. W. Schediwy, K. Grainge, "Simultaneous Transfer of Stabilized Optical and Microwave Frequencies Over Fiber," *IEEE Photonics Technology Letters*, vol. 30, pp. 87-90, 2018.
- [20] G. Marra et al. "Towards an international optical clock comparison between NPL and SYRTE using an optical fibre network," Poster, presented at 28<sup>th</sup> EFTF, Neuchâtel, Switzerland, 2014. Available: [https://geant3plus.archive.geant.net/opencall/Optical/Documents/ICOF\\_final\\_EFTF%202014%20Poster%20v4%200%20b.pdf](https://geant3plus.archive.geant.net/opencall/Optical/Documents/ICOF_final_EFTF%202014%20Poster%20v4%200%20b.pdf).
- [21] P. Delva et al., "Test of Special Relativity Using a Fiber Network of Optical Clocks," *Phys. Rev. Lett.* vol. 118, 221102, 2017.
- [22] N. R. Newbury, P. A. Williams, and W. C. Swann, "Coherent transfer of an optical carrier over 251 km," *Optics Letters*, vol. 32, pp. 021101/1-25, 2007.
- [23] G. Grosche, et al., Transmission of an Optical Carrier Frequency over a Telecommunication Fiber Link, Conference on Lasers and Electro-Optics/Quantum Electronics and Laser Science Conference and Photonic Applications Systems Technologies Optical Society of America, paper no. CMKK1, 2007.
- [24] P. Krehlik, Ł. Śliwczynski, Ł. Buczek and M. Lipiński, "Fiber optic joint time and frequency transfer with active stabilization of the propagation delay," *IEEE Trans. Instrum. Meas.*, vol. 61, pp. 2844-2851, 2012.
- [25] P. Krehlik, Ł. Śliwczynski, Ł. Buczek, J. Kołodziej and M. Lipiński, "Ultrastable long-distance fibre-optic time transfer: active compensation over a wide range of delays," *Metrologia*, vol. 52, pp. 82-88, 2015.
- [26] Ł. Śliwczynski, et al., "Calibrated optical time transfer of UTC(k) for supervision of telecom networks," *Metrologia*, vol. 56, pp. 1-13, 2019.
- [27] Ł. Śliwczynski, P. Krehlik, Ł. Buczek and H. Schnatz, "Picoseconds-Accurate Fiber-Optic Time Transfer With Relative Stabilization of Lasers Wavelengths," *Journal of Lightwave Technology*, vol. 38, pp. 5056-5063, 2020.
- [28] Ł. Śliwczynski, P. Krehlik and K. Salwik, "Modeling and optimization of bidirectional fiber-optic links for time and frequency transfer," *IEEE Trans. Ultrason. Ferroelectr. Freq. Control*, vol. 66, pp. 632-642, 2019.
- [29] M. Amemiya, M. Imae, Y. Fujii, T. Suzuyama, F. Hong, M. Takamoto, "Precise frequency comparison system using bidirectional optical amplifiers," *IEEE Trans. Instr. Meas.*, vol. 59, pp. 632-640, 2010.
- [30] X. Ding, G. Wu, F. Zuo and J. Chen, "Bidirectional optical amplifier for time transfer using bidirectional WDM transmission," *Optoelectronics Letters* vol. 15, pp. 401-405, 2019